Research Article | Vol. 13, No. 4 / 1 Apr 2022 / Biomedical Optics Express 2144
Biomedical Optics EXPRESS

UV surface disinfection in a wearable drug delivery device

ADAM ZREHEN, URI HILI, NOAM WEIL, ORI BEN-DAVID, ANDREI YOSEF, AND BOAZ EITAN*

Eitan Medical, Netanya 4250529, Israel
**boaz.eitan@eitanmedical.com*

Abstract: The advent of recombinant DNA technology fundamentally altered the drug discovery landscape, replacing traditional small-molecule drugs with protein and peptide-based biologics. Being susceptible to degradation via the oral route, biologics require comparatively invasive injections, most commonly by intravenous infusion (IV). Significant academic and industrial efforts are underway to replace IV transport with subcutaneous delivery by wearable infusion devices. To further complement the ease-of-use and safety of disposable infusion devices, surface disinfection of the drug container can be automated. For ease of use, the desired injector is a combination device, where the drug is inside the injector as a single solution combination device. The main obstacle of the desired solution is the inability to sterilize both injector and drug in the same chamber or using the same method (Gamma for the drug and ETO for the injector). This leads to the assembly of both drug container and injector after sterilization, resulting in at least one transition area that is not sterilized. To automate the delivery of the drug to the patient, a disinfection step before the drug delivery through the injector is required on the none-sterilized interface. As an innovative solution, the autoinjector presented here is designed with a single ultraviolet light-emitting diode (UV LED) for surface disinfection of the drug container and injector interface. In order to validate microbial disinfection similar to ethanol swabbing on the injector, a bacterial 3 or 6 log reduction needed to be demonstrated. However, the small disinfection chamber surfaces within the device are incapable of holding an initial bacterial load for demonstrating the 3 or 6 log reduction, complicating the validation method, and presenting a dilemma as to how to achieve the log reduction while producing real chamber conditions. The suggested solution in this paper is to establish a correlation model between the UV irradiance distribution within the disinfection chamber and a larger external test setup, which can hold the required bacterial load and represents a worse-case test scenario. Bacterial log reduction was subsequently performed on nine different microorganisms of low to high UV-tolerance. The procedure defined herein can be adopted for other surface or chamber disinfection studies in which the inoculation space is limited.

1. Introduction

The start of the biological drug revolution can be traced to the early 1970s with the demonstration that isolated genes from one organism could be cloned and expressed in another unrelated organism, a technique now known as recombinant DNA technology [1]. Currently around 30% of all drugs approved by the Food and Drug Administration (FDA) are biologics [2], and biologic targets are expected to increase with the accelerating pace of genomics and proteomics, aided largely by continued advances in DNA sequencing and proteome analysis [3–5]. Biologics have identified targets for treating anemia, cystic fibrosis, growth deficiency, diabetes, and cancers, to name a few [6]. Nonetheless, biologics are considerably more challenging to manufacture than small molecules, being unstable, not entirely characterizable, and strongly process-dependent [7,8]. Moreover, while small-molecule drugs benefit from considerably simpler and convenient oral administration, biologics are susceptible to degradation in the alimentary canal, as well as by

#453270 https://doi.org/10.1364/BOE.453270
Journal © 2022 Received 7 Jan 2022; revised 10 Feb 2022; accepted 10 Feb 2022; published 16 Mar 2022
Corrected: 29 March 2022

Biomedical Optics EXPRESS

other biological barriers such as the skin and mucus. Therefore, they require parenteral delivery, which to date has most commonly been performed by intravenous (IV) injection.

Over the past few years, the soaring interest in biologics has been paralleled by a proliferation of value-based healthcare, which has extended to the patient-drug delivery experience. Given rising healthcare costs, pharmaceutical companies are under increasing pressure to provide parenteral drug administration solutions capable of addressing both patients and healthcare providers. These solutions focus on converting IV administration to either subcutaneous injection or non-invasive routes such as transdermal, oral, nasal, or inhalation. Subcutaneous delivery has already been approved for clinical use for over 100 biologics [2], and its potential integration with wearable drug delivery devices, or "wearable injectors" furthers its value proposition. Unlike manual injection, wearables offer timed treatment initiation, alternating flow rates, patient-controlled boluses, paused injections, and more. Such subcutaneous injectors can replace costly at home infusion care requiring bulky infusion equipment and/or minimize patient length of stay (LOS) in hospitals. In addition to improving bed management efficiency, reduction in the number of inpatient days lessens patient exposure to secondary infection. Moreover, wearables support shorter and more convenient dosing regimens that are more likely to be adhered to compared with invasive IV infusions [9].

Wearable injectors come in three primary configurations differentiated by the filling method. Either the medication is filled at point-of-care into the device, a prefilled primary container is loaded into the device at the point-of-care, or the device is prefilled and preloaded. In all these configurations, maintaining the pharmaceutical company's primary drug container is preferred since most often the regulatory approvals, procurement concerns, costs, as well as chemical interactions have already been established for that container. Therefore, a wearable injector that accommodates an existing drug container can drastically improve time to commercialization. The most widely used primary container is the vial; however, most viable wearable injectors are either limited to cartridges or use special adapters to receive vial-based contents. A recently introduced wearable injector [10] overcomes various design challenges to offer the first prefilled and preloaded vial-based solution. One major obstacle considered is the disinfection of the container surface, which needs to take place just prior to drug delivery. This task would typically be achieved by swabbing the needle puncture site with a 70% ethanol or isopropanol pad [11]; however, the very advantage of a preloaded device makes this surface inaccessible.

In an alternative configuration presented here, the wearable injector contains a single integrated ultraviolet (UV) light emitting diode (LED) for disinfection of the drug container stopper surface and injector interface at the point-of-care (Fig. 1). While ultraviolet germicidal irradiation (UVGI) is widely associated with the disinfection of liquids, in particular drinking water and wastewater [12,13], as well as the disinfection of air in air handling units [14,15], its potential applications for surface disinfection are far wider. Some applications of UV-based disinfection for surfaces have already taken place in the healthcare space. Most prominent are the UVGI generators for whole room disinfection [16], but several scaled down UV disinfection devices have also been proposed. For example, hand-held or portable ultraviolet radiation devices were developed for decontamination of healthcare associated pathogens on tables and miscellaneous items (keyboards, etc.) [17,18], and a disinfection procedure was designed using UV light for safe reuse of ultrasound probes [19]. Nonetheless, few, if any, studies have systematically examined the efficacy of single UV LEDs for small-scale (<1 cm^2) surface disinfection, and no such technology has been demonstrated in a wearable infusion device. UV LEDs are advantageous in that they can be easily integrated, require minimal power, and are dose-programmable. Nonetheless, the greatest challenge to overcome is the validation of microbial disinfection, which is complicated by the non-uniform irradiance occurring as such confined dimensions and the inability to inoculate it with the bacterial load required for the log reduction.

Biomedical Optics EXPRESS

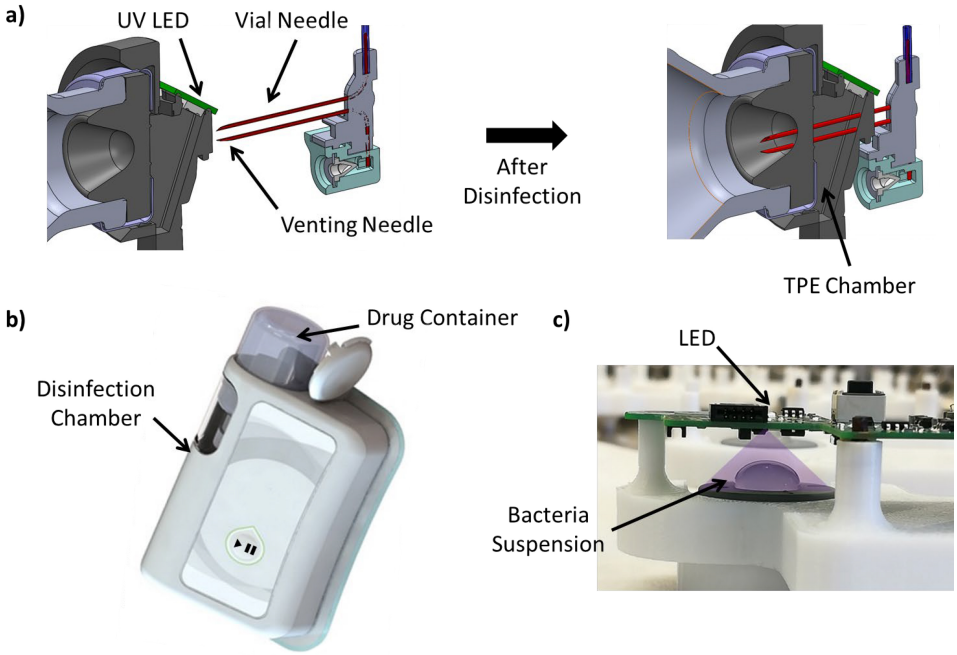

Fig. 1. Wearable infusion device and validation setup. a) computer aided design (CAD) model of the disinfection chamber before and after disinfection, showing the interface between the device and the stopper of the drug container. The vial and venting needles are shown in their positions prior to and after insertion into the drug container via the thermoplastic elastomer (TPE) chamber, which occurs after UV surface disinfection. b) Illustration of the infusion device with the glass drug container partially inserted. The disinfection chamber is situated at the interface of the drug container and pump, hidden behind the outer plastic molding. c) Disinfection validation setup showing the position of the LED, mounted to a printed circuit board (PCB) and test substrate. An illustration of the UV light was superimposed on the captured image.

The UV surface disinfection validation studies presented in the literature are commonly implemented by one or more of the following methods: i) swabbing of the surface in its native state, that is, without direct inoculation of the surface with a foreign challenge organism [16,19–21], ii) inoculation and complete drying of a vegetative or non-vegetative suspension on the test surface [22–25], iii) growth of a biofilm layer on the test surface [26], or iv) inoculation and spreading of a vegetative organism in its wet state [27]. The first method best captures realistic contamination scenarios but does not present a significant challenge to the UV disinfection system since the device undergoes ethylene oxide (EtO) sterilization before packaging. Therefore, the latter three methods were investigated for use in this disinfection validation study with nine different bacteria as challenge organisms. Unlike the aforementioned studies, where disinfection took place on surfaces that could be easily inoculated with a sufficient initial bacterial load, an enclosed disinfection chamber significantly limits the inoculation volume and limits the process success prospects. Importantly, given the proximity of the LED to the targeted disinfection surfaces in the infusion device, it was necessary to first model the UV irradiance distribution, which varies significantly with distance and angle from the source. In this way, an alternative geometrically equivalent setup was designed based on the weakest dose, and thus the "local" survivability of bacteria as opposed to the "bulk" survivability over the entire exposure area was assessed. The full methodology and log reduction testing are described herein.

Biomedical Optics EXPRESS

2. Materials and methods

2.1. Modelling the UV irradiance

An experimental setup for log reduction was designed according to the modelled UV irradiance distribution in the UV chamber of the wearable infusion pump. To understand the need for the model and creation of a separate log reduction setup, it is necessary to first detail the mechanism and geometry of the disinfection apparatus. The wearable infusion pump consists of a UV chamber interfacing the pump's sterilized fluid path and the unsterilized drug container that originates from the outside environment (Fig. 1). The vial contents are delivered to the pump via a hypodermic needle, and an additional needle is used for venting. The needles are part of the sterilized pump. The only non-sterilized interfaces are the outer septum from the device side and the vial stopper surface. Before the needles can be deployed across the UV chamber and puncture the stopper, these two surfaces must be UV-disinfected. More specifically, the needle insertion sites through these two surfaces need to be disinfected rather than the entire chamber. These insertion sites can be accurately designed within a measurable tolerance, and the UV LED is positioned to capture both surfaces in a single exposure. These two surfaces are compact (<1 cm^2) and do not allow the freedom to inoculate an initially high bacterial load aiming for a 3 or 6 log reduction (such as $10^8 - 10^9$ CFU/mL), without contaminating non-exposed surfaces to UV irradiance during the disinfection process. For example, a 0.2 milliliter of inoculant will come in contact with the entire disinfection chamber surface, while the surface of interest is less than 20% of the total surface. Those surfaces eventually hold viable bacteria throughout the disinfection process, which, after extraction and incubation, evolve into colonies. Those colonies cannot be excluded from the summative log reduction counting hence causing the validation effort to fail.

The UV irradiance varies according to three geometric parameters: the distance from the LED, the angle the light makes with the incident surfaces, and the direction of the light emanating from the LED. Therefore, some regions in the chamber receive higher UV exposure than others, varying even by over 9-fold between needle insertion sites. Consequently, any log reduction experiment performed directly in the UV chamber would only provide an estimate of the bulk survivability of bacteria and would not address the local survivability of bacteria at specific insertion sites. The experiment would be biased by the much lower survivability of bacteria exposed to higher doses. Instead, measurement of the local survivability of bacteria at the most challenged insertion site (receiving the lowest UV dose) represents a worse-case test condition than a bulk analysis. To determine the weakest UV dose in the device chamber, the UV irradiance, defined as the radiant flux per surface area, was modelled according to the standard equation for light emanating from a source, in this case a Lambertian emitter, which is projected onto an angled surface [29–31]:

$$E = I * \frac{cos^m(\theta)}{r^2} \quad [mW/cm^2] \tag{1}$$

where, I is the absolute intensity of the source (mW/sr), r is the distance (cm) to the surface, and θ is the angle between the surface normal and the incident light. Here, $I = I_{max} * I_{rel}(\varphi)$ where I_{rel} is the relative intensity, varying with angle φ from the source, and I_{max} is the maximum intensity (mW/sr). To achieve a higher accuracy luminescent model, $I_{rel}(\varphi)$ can be expressed by a fitting curve in the shape of [29] :

$$I(\varphi) = (c(0) + c(1)\varphi + c(2)\varphi^2 + c(3)\varphi^3 + c(4)\varphi^4)\cos^m(\varphi) \tag{2}$$

where the coefficients can be determined empirically. Due to available data and simplicity considerations, instead of using Eq. (2), the intensity curve $I(\varphi)$ provided in the LED specifications was numerically converted and incorporated to our irradiance model in Eq. (1).

Biomedical Optics EXPRESS

The exponential "m" is a dimensionless number reflecting the LED viewing angle, typically greater than 30°, and defined as [29]:

$$m = \frac{-\ln 2}{\ln\left(\cos\left(\varphi_{\frac{1}{2}}\right)\right)} \tag{3}$$

In the described UV LED, m equals approximately 1, representing a perfect Lambertian, making its contribution negligible, and hence it was omitted from calculations based on Eq. (1). While in principle the intensity can vary both with the polar angle and azimuthal angle, the intensity is taken to be constant as a function of the latter, in accordance with the LED specifications (Fig. 2). The value for θ is calculated as the inverse cosine of the dot product of the unit vector in the direction of the light ray, $\vec{I}$, and the unit normal vector, $\vec{N}$, of the surface plane. This equation is valid in the far-field, for distances of r greater than five times the greatest dimension of the source [32,33]. The dose at a specific wavelength $H_e(\lambda)$ is subsequently calculated from the irradiance and disinfection time as [28,34]:

$$H_e(\lambda) = E(\lambda)\Delta t \quad [mJ/cm^2] \tag{4}$$

where Δt is the disinfection time in units of seconds and $E(\lambda)$ is the irradiance in mW/cm^2. Validation of the UV irradiance model, i.e., Eq. (1), was implemented by first measuring the light irradiance at different distances and angles away from the UV source using an XYZ stage fitted with a UV sensor (GenUV GUVCL-T21) that converts irradiance to voltage. Following mapping with the XYZ stage, the data was subsequently fitted to Gaussian profiles as a function of z from the source. As the XYZ stage axis is imperfectly aligned with the LED, the maximum measured irradiance was taken to be at the center of the LED, and the Gaussian fittings were offset accordingly (shown in Fig. 3(a)). Subsequently, the linearity of the measured irradiance, E, was assessed as a function of the right-hand side of Eq. (1), $\frac{\cos(\theta)}{r^2}$. As shown in Fig. 3(b), the relationship is linear, implying that the chosen model for UV irradiance is accurate at this working distance.

The UV irradiance distribution in the UV chamber is presented in Fig. 3(c). Also considered was the maximum expected needle displacement along the x and y axes, as determined by a mechanical design tolerance analysis. The needle position in the CAD design was varied along the x-axis and y-axis separately until mechanical contact occurred between the needle and guide-holes or between the needle housing and track. The largest tolerance in either axis was used to fit a circular region of specific diameter for each of the four needle insertion sites. The weakest average insertion site irradiance was extracted from the model and used to design the validation setup. Using a 2 mW LED operating for 60 seconds, for example, the minimum average insertion site dose would be around 142 mJ/cm^2, occurring at the lower insertion site on the stopper. The other insertion site average doses are 1040 mJ/cm^2 (septum, top), 322 mJ/cm^2 (septum, bottom), and 170 mJ/cm^2 (stopper, top). The weakest single point is slightly lower than the weakest insertion site average, at around 127 mJ/cm^2, whereas the strongest single point is 1250 mJ/cm^2, occurring within the top insertion site in the septum, which is over 9-times greater than the weakest single point dose. The exact LED power and duration is set according to the microbial disinfection results.

2.2. Design of validation setup

To emphasize the challenge at hand, the design of the geometrically equivalent validation setup was motivated by the inability to demonstrate 3 or 6 log reduction within the medical device itself. The claim of equivalency comes from the analytical modelling of the device's UV chamber, using the proposed irradiance model (Eq. (1)) incorporated with the LED manufacturing specifications (Fig. 2(b)) and the disinfected surfaces orientation (described in Fig. 3(c)). This modelling

Biomedical Optics EXPRESS

a)

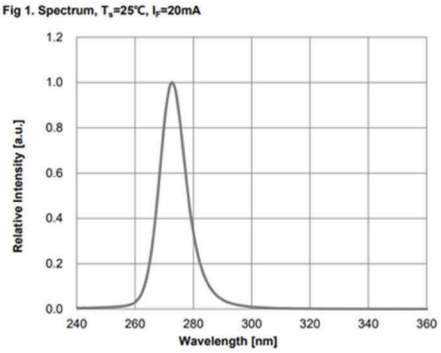

b)

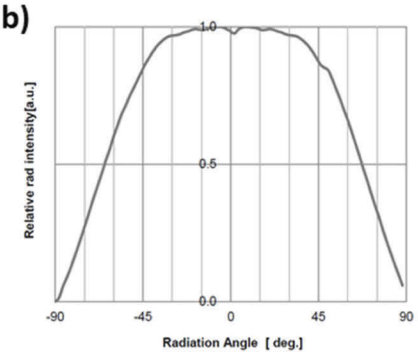

Performance Characteristics

c)

Table 1. Electro-Optical characteristics at 20mA

(T_s=25℃, RH=30%)

Parameter	Symbol	Value	Unit
Peak wavelength [1]	λp	275	nm
Radiant Flux[2]	Φe[3]	2.0	mW
Forward Voltage [4]	VF	6.0	V
Spectrum Half Width	Δ λ	11	nm
Radiant Angle	2Θ1/2	125	deg.

Fig. 2. UVC LED specifications. a) Relative intensity curve as a function of wavelength, with a peak wavelength of 275 nm, and half width of 11 nm. b) Relative intensity curve as a function of viewing angle. Intensity is reduced by 50% for a half viewing angle ($\varphi_{1/2}$) of 62.5°. c) Supplementary electro-optic data. LED efficiency, also described as "wall plug efficiency" (WPE) can be calculated according to the relation of $\eta_e = \frac{\Phi_e(\lambda)}{P}$ [28]. The total flux $\Phi_e(\lambda)[mW]$ at a given wavelength is provided by the manufacturer and equals to 2 mW. The electrical P $[mW]$ equals $V \cdot I$ hence $\eta_e = 1.67\%$.

provided the irradiance mapping inside the chamber, and most importantly exposed the weakest regions where a sufficient dose takes the longest amount of time to be achieved. By identifying those sparse regions, a test setup simulating those regions can be established, allowing us to perform a UV log reduction experiment, calculate the applied effective dose on the disinfected surface and claim equivalency with respect to the infusion device.

For experimental simplicity and robustness, in the validation setup the UV LED was placed perpendicular to the surface of the test substrate, as shown in Fig. 1(c). Using the irradiance model described in Eq. (1), the validation setup was designed to deliver an average dose about 20% less (as a safety margin) than the weakest dose in the UV chamber (117 mJ/cm^2 versus 142 mJ/cm^2) in the device. Since the irradiance varies with the inverse-square of the distance to the source, this was done by simply adjusting the distance, z, of the LED to the test surface, while maintaining the same inoculation area (a circular area of around 10.6 mm in diameter). In the chosen geometry, the LED is positioned 9 mm from the test surface, and the exposure area extends up to an angle of $\theta = 30°$ with the test surface. Since the resulting irradiance profile in the validation setup is also non-uniform, it is possible that the log reduction experiment is again biased, but this time non-favorably, by the higher survivability of bacteria at the edges of

Biomedical Optics EXPRESS

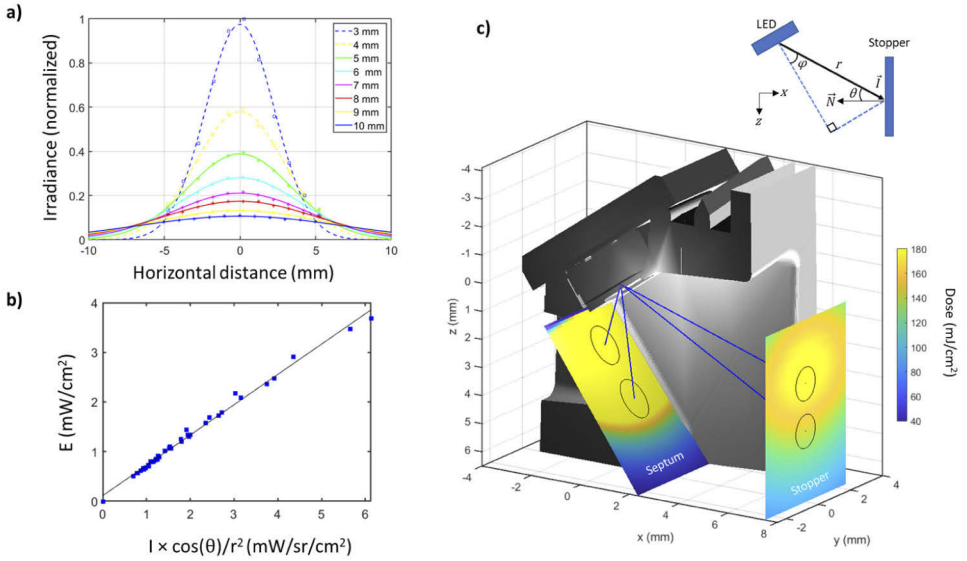

Fig. 3. UV irradiance model. a) Raw data measurements of UV irradiance from a single LED positioned 3 to 10 mm normally from the UV sensor and varied from −5 to 5 mm orthogonally along one axis for a total of 11 points at each distance. The data was fitted to Gaussian functions. b) Relationship between measured irradiance and relevant geometric parameters: the distance, r, from the source, and the angle of the incident light with the surface, θ. The plotted points are derived from the Gaussian fittings in the range of 4 to 10 mm. The line of best fit was assessed for N = 48 samples. c) Irradiance distribution on the septum and stopper walls, solved in MATLAB. The CAD model was superimposed on the irradiance model for visualization. The needle insertion sites are indicated by the circles. The coordinate system is shown above the plot.

the inoculation site. It would be near impossible to construct a uniform irradiance profile at the distance under consideration given the non-isotropic nature of the light source. Moreover, it is assumed that the UV radiation impacting the bacterial DNA is equally effective at all angles (i.e., the orientation of the DNA is random). The validation was repeated separately for each test material (stopper and septum), since each possesses unique surface finish/roughness, hence reflectivity, which can impact the average delivered dose [35].

2.3. Selection of test bacteria

The selection of test bacteria depends on the intended use of the medical device and risk of transmitting disease. The FDA classifies low-level disinfection as a process that kills most vegetative bacteria, some viruses, and some fungi, but not mycobacteria or bacterial spores [36]. Although a low-level disinfection requirement is appropriate given the expectation of low microbial contamination for a primarily sterile non-reusable device, testing was implemented under more stringent assumptions using both moderately and highly UV tolerant microorganisms at high concentration. The moderately UV tolerant microorganisms were tested for 6-log reduction and include unmixed suspensions of *Pseudomonas aeruginosa* (ATCC 9027), *Staphylococcus aereus* (ATCC 6538), *Escherichia coli* (ATCC 8739), *Micrococcus luteus* (ATCC 10240), *Klebsiella pneumonia* (ATCC 4352), and *Klebsiella aerogenes* (ATCC 51697). The highly UV tolerant microorganisms were tested for 3-log reduction and include *Bacillus subtilis* spores (ATCC 5230), *Bacillus pumilus* spores (ATCC 27142), and *Deinococcus radiodurans* (ATCC 13939). Note that to date there is no FDA standard on UV surface disinfection, and the choice of

Biomedical Optics EXPRESS

log reduction can be modified according to the specific risk tolerance. It is worth emphasizing that any vegetative bacteria are likely to be eradicated by UV doses suitable for sterilizing spores [37]. As such, spore suspensions are common candidates for UV surface disinfection studies [22,23].

Justification for the selection of the vegetative microorganisms is made mainly based on their prevalence and risk to humans. *Pseudomonas aeruginosa* is a common Gram-negative bacterium that can cause disease in humans and can be found in most man-made environments, including hospitals [38]. *Staphylococcus aureus* is the second most isolated bloodstream pathogen and responsible for half a million hospitalizations and 50,000 deaths per year in the USA alone [39]. *Escherichia coli*, as the best characterized organism on earth and studied extensively in UV disinfection [40], represents an ideal reference organism and can cause life-threatening illness. *Klebsiella pneumonia* is a bacterium that has become increasingly resistant to antibiotics, rendering infections by these strains very challenging to treat [41]. Lastly, *Micrococcus luteus* is a generally harmless saprophyte that is found ubiquitously but can be opportunistic pathogens for the immunocompromised [42].

Another important parameter in the selection of bacteria is the bacterial substrate. UV disinfection testing is commonly implemented using spores, since spores represent the greatest microbial challenge, but also because spores are unaffected by drying and the resulting high osmotic pressure in the surrounding environment. As was observed experimentally (data not shown), the concentration of a vegetative solution dried on the test substrate is reduced significantly by drying. This complicates the testing procedure especially when the surface area of the substrate is small, since a concentrated bacteria solution on the order of 10^8 to 10^9 cfu/ml will be compacted into a relatively thick, UV-impenetrable film. By comparison, the study presented by Chen et al. (2019) used 200 µl aliquots of *Staphylococcus aureus* dried over a 100 cm^2 area, whereas the test substrate used in the current validation method is only 0.8 cm^2 for the same aliquot volume [26]. A similar limitation can be inferred for biofilms, i.e., the surface area of the substrate is insufficient to support a biofilm with realistic thickness. Moreover, drying times can vary between samples and drying is non-uniform, which results in significant variability in the log reduction results. Therefore, UV disinfection of the spore species was conducted in the dry state, whereas UV disinfection of the vegetative bacteria was conducted in the wet state.

2.4. Log reduction testing

Prior to inoculation, all materials were washed with sterile PBS and dried. The test materials (stopper and septum) were inoculated with 200 µl of microorganism suspension, either dried for several hours (spores) or kept in the wet state (vegetative bacteria) and were UV-treated. The suspension was pipetted onto the surface in the form of a droplet, which stayed intact due to the hydrophobicity of the elastomeric surface. Three samples were treated at each dose up to 300 mJ/cm^2 with dose intervals of typically around 30-100 mJ/cm^2 depending on the expected resolution to capture the log reduction dynamics. The positive control was also repeated in triplicate. The samples that were UV-treated as well as PC and negative control (NC) samples were each transferred to a test tube containing 30 mL of PBS and vortexed for 1 for minute. The contents of all tubes were serially diluted, the appropriate dilutions were filtered, and the membranes were transferred to MacConkey Agar plates. All plates were incubated at 30-35° for up to 3 days, and the individual colonies were counted for calculation of the log reduction, using the following equation:

$$Log\ Reduction = \log_{10}\frac{A}{B} \tag{5}$$

where A is the average colony count of the positive control (average of 3 samples), and B is the colony count of the disinfected sample (average of 3 samples). The data was subsequently fitted to exponential decaying functions using nonlinear minimization (Nelder-Mead method).

Biomedical Optics EXPRESS

The choice of an exponential fitting ultimately depends on the quality of the fitting with the observations, but many studies of UV surface, water, and even air disinfection show exponential or sigmoidal dose dependency. Exponential behavior is consistent with the application of ionizing radiation, including UV radiation, where the death rate of the microorganism is described as a single-unit action [37,43]. When the death of a microorganism is the result of a cumulative effect, the curve is sigmoidal [44]. An initial lag phase with a lower rate of deactivation may be present if a certain minimum dose is required to impart any detrimental effect, as observed in early surface disinfection studies of *Bacillus anthracis* [45]. If the microbial inactivation rate drastically decreases with increasing dose, a tailing phase may appear, which could be attributed to an aggregation of microorganisms (or microorganisms that physically shield others) or the existence of a resistant subpopulation [46,47].

3. Results and discussion

The log reduction versus dose summary for the nine tested microorganisms is presented in Fig. 4(a), and selected graphs of the raw data fitted to exponential functions are presented in Fig. 4(b). The choice of a single exponential fitting appears to be correct for most of the experiments, which can be qualitatively inferred by the proximity of the data points to the fitted function. While the *Deinococcus radiodurans* data deviates somewhat from exponential, the reduction can still be extracted. To calculate the log-reduction dose for each microorganism, the intersection of the fitted exponential function with the required reduction level (dashed line in Fig. 4(b)) was determined. The decimal reduction time (D-value) was subsequently calculated as the required dose divided by the log reduction (either 6 or 3 log). As can be seen in the raw data measurements, typically the standard deviation between repeats was minimal, and any error may in part be explained by the variance in droplet positioning relative to UV LED position. Any deviations from perfect center result in a lower average dose. In the wet state, *Staphylococcus aureus* was the easiest to kill and *Deinococcus radiodurans*, which is known to be highly effective

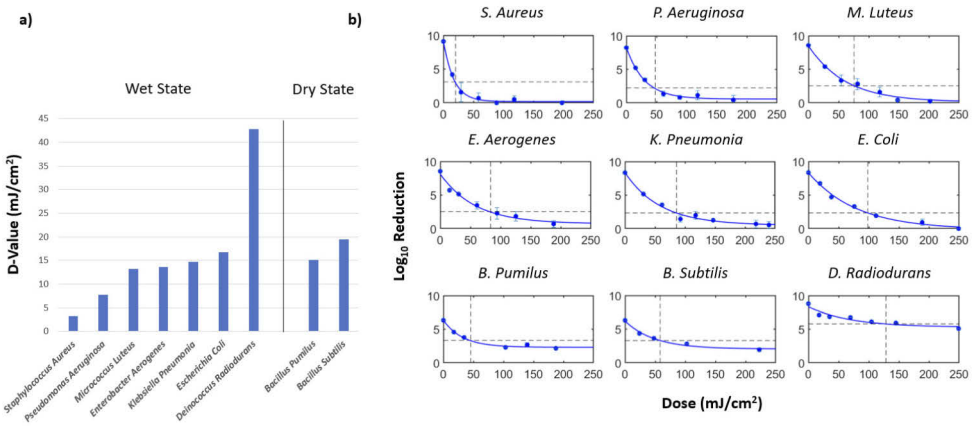

Fig. 4. Log reduction results. a) Comparison of D-values (dose per log reduction) for all tested microorganisms on the stopper surface. The vegetative species were tested in the wet state, while the spores were tested in the dry state. b) Selected log-reduction graphs showing log reduction versus dose. Each raw data point is an average of three measurements, and the error bar represents one standard deviation. The data was fitted to single exponential functions. The horizontal dashed line represents the required reduction level (either 3 or 6 log), and the required dose at that level is indicated by the intersection with the vertical dashed line. The axis is zoomed in from 0 to 250 mJ/cm^2, and in some cases, there are unseen datapoints (following the exponential trend) outside of this window.

Biomedical Optics EXPRESS

at withstanding lethal and mutagenic damaging agents [48], was the hardest to kill. The two spore species yielded a roughly 30% difference in D-value.

As mentioned, the vegetative bacteria suspension was UV-exposed in the wet state, so there was some uncertainty regarding the killing effectiveness relative to a dried substrate. The surface tension causes the droplet to protrude closer to the LED, by up to about 2.5 mm at the center. Additionally, the dose is affected by the reflectivity and absorbance of the growth medium [35] and for more dense microbial suspensions the absorbance will increase. Therefore, the bacteria at the bottom of the droplet will be obscured by the dense bacteria suspension on top. Importantly, some of the tested bacteria, such as *E. coli*, was as challenging or even more challenging to kill than the highly UV-tolerant spores in the dry state. This contradicts the general expectation of higher spore survivability against UV [37] . In studies of log inactivation of these bacteria in water, the spores were significantly more UV-resistant [49]. This difference is likely ascribed to the layering of the bacteria, as well as the loading concentration of the spores relative to the vegetive bacteria (10^6–10^7 cfu/ml versus 10^8–10^9 cfu/ml). Nonetheless, for validation purposes, the ranking of microorganism UV-tolerance is less critical, and the wet state represents a worse-case, albeit unlikely scenario.

4. Conclusions and summary

Unlike liquid disinfection of a drug container, which is susceptible to human error/forgetfulness, automated surface disinfection using UV light can be validated and controlled. In this study, a unique method was described for UV validation and tested on nine organisms including two spore species. The primary goal of this paper is to address a problem that originated from design and intended use aspects of an on-body injector, using automated surface disinfection by UVC technology. The small size of the disinfection surfaces required an alternative, equivalent test setup based on modelling and mapping the worst-case disinfection sites. The proposed solution successfully enables reduction testing and can be used to overcome future limitations.

It is worth emphasizing that common liquid disinfectants such as ethanol and isopropanol are not recommended as high-level disinfectants for spores by the Center for Disease Control (CDC) because of their inability to inactivate bacterial spores [11]. Moreover, several studies have shown high spore survivability when subjected to ethanol treatment [50]. UV light, on the other hand, will eradicate many spores, such as *Bacillus subtilis* [51], given sufficient irradiation. The validation strategy presented here was designed to measure the "log kill" or log reduction and does not consider actual contamination levels present on the device. The bacteria load tested is highly unlikely, as contact studies of other common disinfection surfaces of interest show substantially lower contamination levels [19,20] . The medical device at hand is a commercial, single use injector that utilizes an off-the-shelf UV LED. Cost-benefit considerations were important to eventually select a specific UV LED, such that the emission profile, intensity, power rating and wavelength serve the best tradeoffs. Design improvements, such as micro-lenses equipped to the LED for emission enhancement, or reflective coatings of both disinfected surfaces to increase irradiance, can be considered to achieve better results in the device. A future optimization study for identifying the best wavelength to pick based on a known group of pathogens as suggested in [52–55] can be highly beneficial, by enabling a reduction of the LED exposure period in accordance with the highest UV tolerant bacteria.

Funding. Eitan Medical.

Acknowledgments. The authors acknowledge the support of Aminolab (Rehovot, Israel) in preparing and growing the test microorganisms and performing colony counting.

Disclosures. The authors have no conflicts of interest to disclose.

Data Availability. Data are available upon request from the corresponding author.

Biomedical Optics EXPRESS

References

1. M. S. Kinch, "An overview of FDA-approved biologics medicines," Drug Discovery Today **20**(4), 393–398 (2015).
2. A. C. Anselmo, Y. Gokarn, and S. Mitragotri, "Non-invasive delivery strategies for biologics," Nat. Rev. Drug Discovery **18**(1), 19–40 (2019).
3. J. Shendure and H. Ji, "Next-generation DNA sequencing," Nat. Biotechnol. **26**(10), 1135–1145 (2008).
4. J. A. Alfaro, P. Bohländer, M. Dai, M. Filius, C. J. Howard, X. F. van Kooten, S. Ohayon, A. Pomorski, S. Schmid, A. Aksimentiev, E. v. Anslyn, G. Bedran, C. Cao, M. Chinappi, E. Coyaud, C. Dekker, G. Dittmar, N. Drachman, R. Eelkema, D. Goodlett, S. Hentz, U. Kalathiya, N. L. Kelleher, R. T. Kelly, Z. Kelman, S. H. Kim, B. Kuster, D. Rodriguez-Larrea, S. Lindsay, G. Maglia, E. M. Marcotte, J. P. Marino, C. Masselon, M. Mayer, P. Samaras, K. Sarthak, L. Sepiashvili, D. Stein, M. Wanunu, M. Wilhelm, P. Yin, A. Meller, and C. Joo, "The emerging landscape of single-molecule protein sequencing technologies," Nat. Methods **18**(6), 604–617 (2021).
5. A. Zrehen, S. Ohayon, D. Huttner, and A. Meller, "On-chip protein separation with single-molecule resolution," Sci. Rep. **10**(1), 15313 (2020).
6. T. Morrow and L. Felcone, "Defining the difference: what makes biologics unique," Biotechnology Healthcare **1**, 24–29 (2004).
7. S. J. Shire, "Formulation and manufacturability of biologics," Curr. Opin. Biotechnol. **20**(6), 708–714 (2009).
8. F. D. Makurvet, "Biologics vs. small molecules: drug costs and patient access," Med. Drug Discovery **9**, 100075 (2021).
9. B. Bittner and J. Schmidt, "Subcutaneous drug delivery devices—enablers of a flexible care setting," Drug Delivery Devices and Therapeutic Systems, Chapter 8 (Elsevier, 2021), 159–179.
10. M. Katz and M. Ratigan, "A vial-based solution for wearable drug delivery," On Drug Delivery **100**, 68–72 (2019).
11. W. A. Rutala and D. J. Weber, Guideline for Disinfection and Sterilization in Healthcare Facilities (2008).
12. C. W. McKinney and A. Pruden, "Ultraviolet disinfection of antibiotic resistant bacteria and their antibiotic resistance genes in water and wastewater," Environ. Sci. Technol. **46**(24), 13393–13400 (2012).
13. Z. Bohrerova and K. G. Linden, "Ultraviolet and chlorine disinfection of mycobacterium in wastewater: effect of aggregation," Water Environ. Res. **78**(6), 565–571 (2006).
14. E. Levetin, R. Shaughnessy, C. A. Rogers, and R. Scheir, "Effectiveness of germicidal UV radiation for reducing fungal contamination within air-handling units," Appl. Environ. Microbiol. **67**(8), 3712–3715 (2001).
15. L. Song, W. Li, A. He, L. Li, T. Li, D. Gu, and H. Tang, "Development of a pulsed xenon ultraviolet disinfection device for real-time air disinfection in ambulances," J. Healthc. Eng. **2020**, 1–5 (2020).
16. K. C. Jelden, S. G. Gibbs, P. W. Smith, A. L. Hewlett, P. C. Iwen, K. K. Schmid, and J. J. Lowe, "Comparison of hospital room surface disinfection using a novel ultraviolet germicidal irradiation (UVGI) generator," J. Occup. Environ. Hyg. **13**(9), 690–698 (2016).
17. M. M. Nerandzic, J. L. Cadnum, K. E. Eckart, and C. J. Donskey, "Evaluation of a hand-held far-ultraviolet radiation device for decontamination of *Clostridium difficile* and other healthcare-associated pathogens," BMC Infect. Dis. **12**(1), 120 (2012).
18. R. C. She, D. Chen, P. Pak, D. K. Armani, A. Schubert, and A. M. Armani, "Lightweight UV-C disinfection system," Biomed. Opt. Express **11**(8), 4326–4332 (2020).
19. G. Kac, M. Gueneret, A. Rodi, E. Abergel, C. Grataloup, N. Denarié, S. Peyrard, G. Chatellier, J. Emmerich, G. Meyer, and I. Podglajen, "Evaluation of a new disinfection procedure for ultrasound probes using ultraviolet light," J. Hosp. Infect. **65**(2), 163–168 (2007).
20. B. M. Andersen, H. Bånrud, E. Bøe, O. Bjordal, and F. Drangsholt, "Comparison of UV C light and chemicals for disinfection of surfaces in hospital isolation units," Infect. Control Hosp. Epidemiol. **27**(7), 729–734 (2006).
21. P. W. Smith, S. Gibbs, H. Sayles, A. Hewlett, M. E. Rupp, and P. C. Iwen, "Observations on hospital room contamination testing," Healthc. Infect. **18**(1), 10–13 (2013).
22. D. W. M. Gardner and G. Shama, "UV intensity measurement and modelling and disinfection performance prediction for irradiation of solid surfaces with UV light," Food Bioprod. Process. **77**(3), 232–242 (1999).
23. M. U. Owens, D. R. Deal, M. O. Shoemaker, G. B. Knudson, J. E. Meszaros, and J. L. Deal, "High-dose ultraviolet C light inactivates spores of Bacillus atrophaeus and Bacillus anthracis sterne on nonreflective surfaces," Appl Biosaf. **10**(4), 240–247 (2005).
24. T. Kim, J. L. Silva, and T. C. Chen, "Effects of UV irradiation on selected pathogens in peptone water and on stainless steel and chicken meat," J. Food Prot. **65**(7), 1142–1145 (2002).
25. L. hua Chen, Y. Li, Y. Qi, S. ni Wang, C. qing Gao, and Y. Wu, "Evaluation of a pulsed xenon ultraviolet light device for reduction of pathogens with biofilm-forming ability and impact on environmental bioburden in clinical laboratories," Photodiagn. Photodyn. Ther. **29**, 101544 (2020).
26. B. Joseph, S. K. Otta, I. Karunasagar, and I. Karunasagar, "Biofilm formation by Salmonella spp. On food contact surfaces and their sensitivity to sanitizers," Int. J. Food Microbiol. **64**(3), 367–372 (2001).
27. G. Messina, S. Burgassi, D. Messina, V. Montagnani, and G. Cevenini, "A new UV-LED device for automatic disinfection of stethoscope membranes," Am. J. Infect. Control. **43**(10), e61–e66 (2015).
28. E. Gramsch, P. Fredes, and U. Raff, "Optical considerations for design of surface disinfection devices based on UV-C LEDs," in OSA Optical Design and Fabrication 2021 (Flat Optics, Freeform, IODC, OFT), paper 120780E (2021).
29. F. tie Wu and Q. lu Huang, "A precise model of LED lighting and its application in uniform illumination system," Optoelectron. Lett. **7**(5), 334–336 (2011).

Biomedical Optics EXPRESS

30. I. Moreno and C.-C. Sun, "Modeling the radiation pattern of LEDs," Opt. Express **16**(3), 1808 (2008).
31. R. J. Becherer and F. Grum, *Optical Radiation Measurements* (Academic Press, 1979), **1**.
32. A. D. Ryer, *The Light Measurement Handbook* (International Light Technologies, 1997).
33. I. Moreno and C.-C. Sun, "LED array: Where does far-field begin?" in *Eighth International Conference on Solid State Lighting* (2008), 7058(2008), p. 70580R.
34. P. Fredes, U. Raff, E. Gramsch, and M. Tarkowski, "Estimation of the ultraviolet-C doses from mercury lamps and light-emitting diodes required to disinfect surfaces," J. Res. Natl. Inst. Stan. **126**, 126025 (2021).
35. J. R. Bolton and K. G. Linden, "Standardization of methods for fluence (UV dose) determination in bench-scale UV experiments," J. Environ. Eng. **129**(3), 209–215 (2003).
36. AAMI, Designing, *Testing, and Labeling Reusable Medical Devices for Reprocessing in Health Care Facilities: A Guide for Medical Device Manufacturers* (2010).
37. W. Kowalski, "Ultraviolet germicidal irradiation handbook: UVGI for air and surface disinfection," in *UV Surface Disinfection* (Springer, 2009), pp. 233–254.
38. M. Bassetti, A. Vena, A. Croxatto, E. Righi, and B. Guery, "How to manage *Pseudomonas aeruginosa* infections," DIC **7**, 1–18 (2018).
39. L. M. Schlecht, B. M. Peters, B. P. Krom, J. A. Freiberg, G. M. Hänsch, S. G. Filler, M. A. Jabra-Rizk, and M. E. Shirtliff, "Systemic Staphylococcus aureus infection mediated by Candida albicans hyphal invasion of mucosal tissue," Microbiology **161**(1), 168–181 (2015).
40. S. Pontrelli, T. Y. Chiu, E. I. Lan, F. Y. H. Chen, P. Chang, and J. C. Liao, "Escherichia coli as a host for metabolic engineering," Metab. Eng. **50**, 16–46 (2018).
41. M. K. Paczosa and J. Mecsas, "Klebsiella pneumoniae: going on the offense with a strong defense," Microbiol. Mol. Biol. Rev. **80**(3), 629–661 (2016).
42. M. Kocur, W. E. Kloos, and Schleifer Karl-Heinz, "The Prokaryotes," in *The Prokaryotes*, M. Dworkin, S. Falkow, E. Rosenberg, and E. Stackebrandt, eds. (Springer, n.d.).
43. D. E. Lea, *Actions of Radiations on Living Cells*, 2nd ed. (Cambridge University, 1962).
44. A. Quintero-Ramos, J. J. Churey, P. Hartman, J. Barnard, and R. W. Worobo, "Modeling of *Escherichia coli* inactivation by UV irradiation at different pH values in apple cider," J. Food Prot. **67**(6), 1153–1156 (2004).
45. D. G. Sharp, "The lethal action of short ultraviolet rays on several common pathogenic bacteria," J. Bacteriol. **37**(4), 447–460 (1939).
46. W. A. M. Hijnen, E. F. Beerendonk, and G. J. Medema, "Inactivation credit of UV radiation for viruses, bacteria and protozoan (oo)cysts in water: a review," Water Res. **40**(1), 3–22 (2006).
47. E. Gayán, S. Monfort, I. Álvarez, and S. Condón, "UV-C inactivation of *Escherichia coli* at different temperatures," Innovative Food Sci. Emerging Technol. **12**(4), 531–541 (2011).
48. J. R. Battista, "Against all odds: the survival strategies of *Deinococcus radiodurans*," Annu. Rev. Microbiol. **51**(1), 203–224 (1997).
49. G. Chevrefils, É. Caron, H. Wright, and G. Sakamoto, "UV dose required to achieve incremental log inactivation of bacteria, protozoa and viruses," IUVA News **8**(1), 38–45 (2006).
50. T. H. Lin, F. C. Tang, P. C. Hung, Z. C. Hua, and C. Y. Lai, "Relative survival of Bacillus subtilis spores loaded on filtering facepiece respirators after five decontamination methods," Indoor Air **28**(5), 754–762 (2018).
51. P. Setlow, "Spores of Bacillus subtilis: their resistance to and killing by radiation, heat and chemicals," J. Appl. Microbiol. **101**(3), 514–525 (2006).
52. Y. Gerchman, H. Mamane, N. Friedman, and M. Mandelboim, "UV-LED disinfection of coronavirus: wavelength effect," J. Photochem. Photobiol., B **212**, 112044 (2020).
53. M. Nakahashi, K. Mawatari, A. Hirata, M. Maetani, T. Shimohata, T. Uebanso, Y. Hamada, M. Akutagawa, Y. Kinouchi, and A. Takahashi, "Simultaneous irradiation with different wavelengths of ultraviolet light has synergistic bactericidal effect on *Vibrio parahaemolyticus*," Photochem. Photobiol. **90**(6), 1397–1403 (2014).
54. H. Woo, S. E. Beck, L. A. Boczek, K. M. Carlson, N. E. Brinkman, K. G. Linden, O. R. Lawal, S. L. Hayes, and H. Ryu, "Efficacy of inactivation of human enteroviruses by dual-wavelength germicidal ultraviolet (UV-C) light emitting diodes (LEDs)," Water **11**(6), 1131 (2019).
55. A. Green, V. Popović, J. Pierscianowski, M. Biancaniello, K. Warriner, and T. Koutchma, "Inactivation of *Escherichia coli*, Listeria and Salmonella by single and multiple wavelength ultraviolet-light emitting diodes," Innovative Food Sci. Emerging Technol. **47**, 353–361 (2018).